ACS Chemical Neuroscience

PURDUE UNIVERSITY

Subscriber access provided by Purdue University Libraries

Letter

The pharmacology of cumyl-carboxamide synthetic cannabinoid new psychoactive substances (NPS) CUMYL-BICA, CUMYL-PICA, CUMYL-5F-PICA, CUMYL-5F-PINACA, and their analogues.

Mitchell Longworth, Samuel D. Banister, Rochelle Boyd, Richard C. Kevin, Mark Connor, Iain S. McGregor, and Michael Kassiou

ACS Chem. Neurosci., **Just Accepted Manuscript** • Publication Date (Web): 09 Aug 2017

ACS Publications

ACS Chemical Neuroscience is published by the American Chemical Society. 1155 Sixteenth Street N.W., Washington, DC 20036

The pharmacology of cumyl-carboxamide synthetic cannabinoid new psychoactive substances (NPS) CUMYL-BICA, CUMYL-PICA, CUMYL-5F-PICA, CUMYL-5F-PINACA, and their analogues

Mitchell Longworth,[a] Samuel D. Banister,[a,b] Rochelle Boyd,[c] Richard C. Kevin,[d] Mark Connor,[c] Iain S. McGregor,[d] Michael Kassiou[a]*

[a]School of Chemistry, The University of Sydney, NSW 2006, Australia; [b]Department of Pathology, Stanford University School of Medicine, Stanford, CA 94305, USA; [c]Department of Biomedical Sciences, Macquarie University, NSW 2109, Australia; [d]School of Psychology, The University of Sydney, NSW 2006, Australia

*Corresponding author

Abstract: Synthetic cannabinoids (SC) are the largest class of new psychoactive substances (NPS), and are increasingly associated with serious adverse effects. The majority of SC NPS are 1,3-disubstituted indoles and indazoles featuring a diversity of subunits at the 1- and 3-positions. Most recently, cumyl-derived indole- and indazole-3-carboxamides have been detected by law enforcement agencies and by emergency departments. Herein we describe the synthesis, characterization, and pharmacology of SCs CUMYL-BICA, CUMYL-PICA, CUMYL-5F-PICA, CUMYL-PINACA, CUMYL-5F-PINACA and related analogues. All cumyl-derived SCs were potent, efficacious agonists at CB_1 (EC_{50} = 0.43–12.3 nM) and CB_2 (EC_{50} = 11.3–122 nM) receptors in a fluorometric assay of membrane potential, with selectivity for CB_1 activation (3.1–53 times over CB_2). CUMYL-PICA and CUMYL-5F-PICA were evaluated in rats using biotelemetry, and induced hypothermia and bradycardia at doses of 1 mg/kg. Hypothermia was reversed by pretreatment with a CB_1, but not CB_2, antagonist, confirming that cumyl-derived SCs are cannabimimetic *in vivo*.

Keywords: cannabinoid, CUMYL-BICA, CUMYL-PICA, CUMYL-PINACA, CUMYL-5F-PICA, CUMYL-5F-PINACA

Introduction. Between 2008 and 2015, 644 new psychoactive substances (NPS) have been reported to United Nations Office on Drugs and Crime (UNODC).[1] Of these, synthetic cannabinoids (SCs) are the largest pharmacological class, representing 32% of all reported NPS.[1] The highly dynamic nature of the NPS market—influenced by user preference, law enforcements efforts, and legal response—has produced hundreds of SCs of increasingly structural diversity, with a general trend towards increased cannabinoid receptor potency.

Following the identification and subsequent prohibition of one of the earliest SCs, JWH-018 (**1**, Fig. 1), other 3-acylindoles, such as XLR-11 (**2**), emerged to replace it. Elaborated indole analogues featuring a carboxylate (e.g. BB-22, **3**) or amide (SDB-006, **4**) linker in place of the carbonyl group soon followed, as well as SCs based on other heteroaromatic cores, such as indazole AKB-48 (**5**). The most prevalent recent SCs are indole- and indazole-3-carboxamides featuring pendant amino acid amides or esters, and various aliphatic, alicyclic, and aromatic substituents at the 1-position, as exemplified by 5F-ADB (**6**) and AMB-FUBINACA (**7**).

Figure 1. Representative synthetic cannabinoid new psychoactive substances.

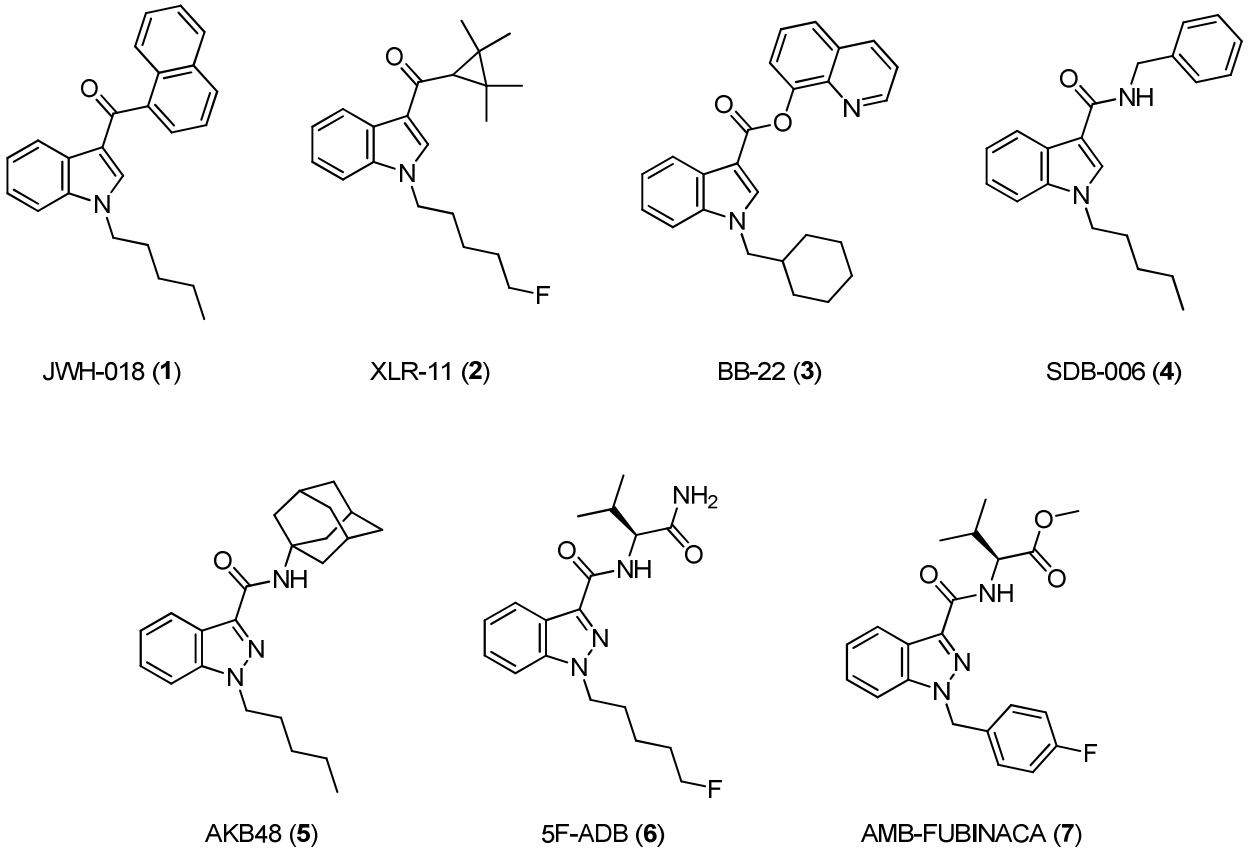

The pharmacology and toxicology of many SCs has been explored, but new structural classes are emerging every year.[2-4] Most recently, SCs featuring a 2-phenylpropan-2-yl (i.e. cumyl) group (**8**–**17**, Fig. 2) have been reported around the world, however, these molecules originate from a patent filed in New Zealand in 2013.[5] CUMYL-5F-PICA (**10**) was identified in Slovenia on 23 September 2014, along with CUMYL-BICA (**8**), and CUMYL-PICA (**9**).[6] Consistent with the trend for terminal fluorination of *N*-pentyl SCs, CUMYL-5F-PINACA (**15**) was identified in Sweden several weeks later,[6] and was reported to the UNODC Early Warning Advisory (EWA) in Luxembourg and the United Kingdom in 2014.[6] Very recently, occupational transdermal exposure to CUMYL-PINACA was reported following a seizure by law enforcement officers in

Slovenia.[7] Despite their prevalence, to date there are relatively few reports in the literature concerning the toxicological effects of these compounds.[8]

To provide analytical and pharmacological data on this emergent class of SCs, we have systematically prepared a library of cumyl-derived indole- and indazole-3-carboxamides featuring the commonly encountered butyl, pentyl, 5-fluoropentyl, 4-fluorobenzyl, and (cyclohexyl)methyl subunits at the 1-position (**8**–**17**).

Figure 2. Cumyl-derived synthetic cannabinoids.

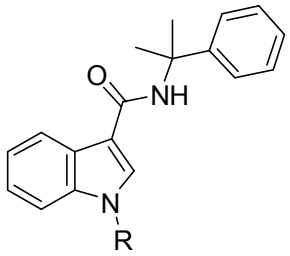

CUMYL-BICA (**8**; R = $(CH_2)_3CH_3$)
CUMYL-PICA (**9**; R = $(CH_2)_4CH_3$)
CUMYL-5F-PICA (**10**; R = $(CH_2)_5F$)
CUMYL-FUBICA (**11**; R = 4-FBn)
CUMYL-CHMICA (**12**; R = CH_2Cy)

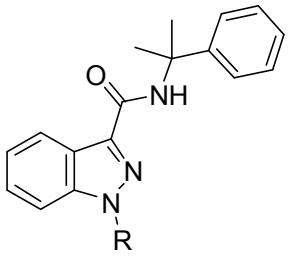

CUMYL-BINACA (**13**; R = $(CH_2)_3CH_3$)
CUMYL-PINACA (**14**; R = $(CH_2)_4CH_3$)
CUMYL-5F-PINACA (**15**; R = $(CH_2)_5F$)
CUMYL-FUBINACA (**16**; R = 4-FBn)
CUMYL-CHMINACA (**17**; R = CH_2Cy)

Results and discussion

The synthesis of indole- (**8**–**12**) and indazole-3-carboxamides (**13**–**17**) is shown in Figures 3 and 4, respectively. As depicted in Figure 3, treatment of indole (**18**) with the appropriate alkyl bromide, followed by trifluoroacetic anhydride, afforded 1-alkyl-3-(trifluoroacetyl)indole intermediates **19**–**23** from a convenient one-pot procedure. Hydrolysis of the trifluoroacetyl group by sodium hydroxide in refluxing aqueous methanol provided carboxylic acids **24**–**28**,

which were subsequently coupled with cumylamine using EDC/HOBt, and furnished the desired cumyl-carboxamides **8**–**12**.

Figure 3. Synthesis of cumyl-derived indole-3-carboxamides.[a]

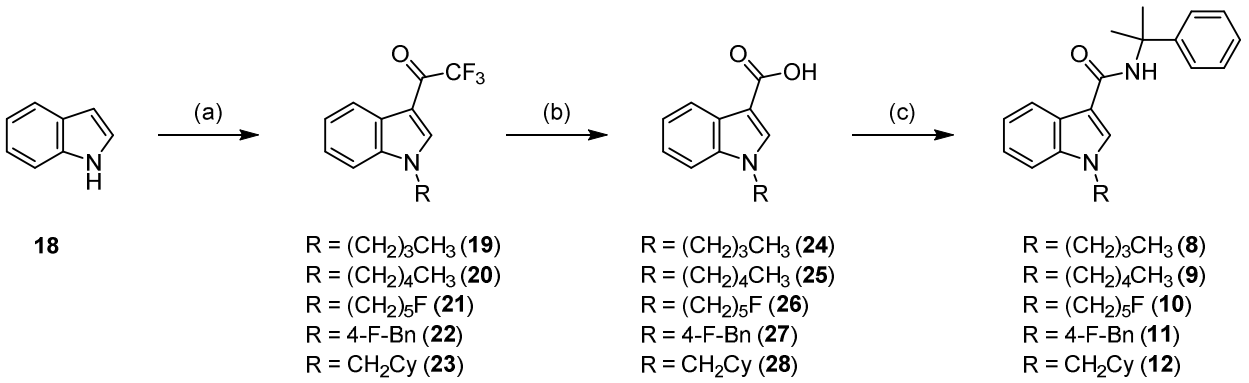

[a]Reagents and conditions: (a)(i) NaH, RBr, DMF, 0 °C-rt, 1 h, (ii) $(CF_3CO)_2O$, rt, 1 h (72-94%); (b) 1 M aq. NaOH, MeOH, reflux, 18 h (67-88%); (c) cumylamine, EDC·HCl, HOBt, DIPEA, DMSO, rt, 14 h (67-80%).

The synthesis of indazoles **13**–**17** is outlined in Figure 4, beginning with alkylation of methyl 1*H*-indazole-3-carboxylate (**29**). Previous studies had demonstrated the role of base in the regiochemical outcome of this alkylation.[9] In order to minimize formation of undesired 2-alkyl-2*H*-indazole-3-carboxylate by-products, **29** was deprotonated with potassium *tert*-butoxide, and treated with the appropriate alkyl bromide to give almost exclusively the 1-substituted 1*H*-indazole-3-carboxylates **30**–**34**. Saponification of the ester group was achieved using sodium hydroxide in aqueous methanol, thereby providing 1-alkyl-1*H*-indazole-3-carboxylic acids **35**–**39**. Coupling of **35**–**39** with cumylamine using EDC/HOBt produced cumyl-carboxamide indazoles **13**–**17**.

Figure 4. Synthesis of cumyl-derived indazole-3-carboxamides.[a]

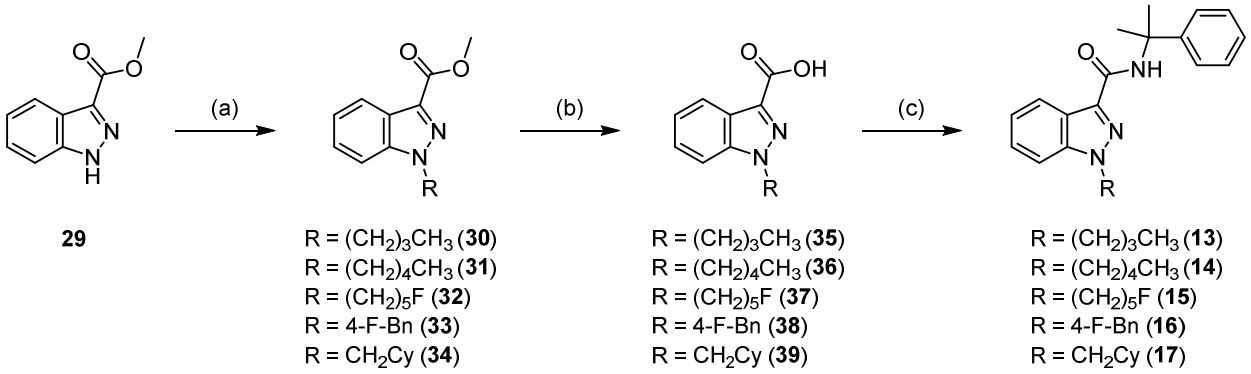

[a]Reagents and conditions: (a)(i) KO^{t}Bu, RBr, THF, 0 °C-rt, 48 h (65-84%%); (b) 1 M aq. NaOH, MeOH, reflux, 18 h (81-91%); (c) cumylamine, EDC·HCl, HOBt, DIPEA, DMSO, rt, 14 h (71-88%).

The synthesized indole and indazole cumyl-carboxamides **8**–**17** were screened at CB_1 and CB_2 receptors using a fluorometric imaging plate reader (FLIPR) assay to identify structure-activity relationships (SARs) for this class, and enable comparisons to other classes of prevalent SCs. The activities of **8**–**17** at CB_1 and CB_2 were compared to the low efficacy $CB_{1/2}$ Δ^9-tetrahydrocannabinol (Δ^9-THC), and the efficacious $CB_{1/2}$ agonist CP 55,940, in an assay of CB receptor-dependent membrane hyperpolarization (Table 1). The assay used murine AtT20-FlpIn neuroblastoma cells stably expressing human CB_1 or CB_2 receptors. Activation of CB receptors resulted in opening of endogenous G protein-gated inwardly rectifying potassium channels (GIRKs) that produced a hyperpolarization of the cells which was reflected in a decrease in the fluorescence of a proprietary membrane potential dye.

The maximum effects of Δ^9-THC and **8**–**17** were normalized to a maximally efficacious concentration of CP 55,490. Data for each experiment were normalized to the change in fluorescence produced by a maximally effective concentration of CP 55,940 (1 μM). CP 55,940 (1 μM) decreased fluorescence by 29.6 ± 0.9 % in CB_1-expressing cells, and 29.7 ± 1.1 % in CB_2-expressing cells (n = 26 each). None of **8**–**17** produced a significant change in the membrane potential of wild type AtT-20 cells (n = 6 each, data not shown), which do not express CB_1 or CB_2 receptors. Consistent with a predominant coupling of CB_1 and CB_2 receptors to G_i/G_o family G proteins, the effects of **8**–**17** were abolished by overnight treatment of the cells with pertussis toxin (200 ng/mL), which blocks the coupling of GPCR to G_i/G_o family G proteins (n = 3 each, Table S2, Supporting Information).

Table 1. Functional activity of Δ^9-THC, CP 55,940, JWH-018, and novel SCs **10**–**25** at CB_1 and CB_2 receptors.

Compound	hCB_1	hCB_1	hCB_2	hCB_2	CB_1 sel.*
	pEC_{50} ± SEM (EC_{50}, nM)	Max ± SEM (% CP 55,940)	pEC_{50} ± SEM (EC_{50}, nM)	Max ± SEM (%CP 55,940)	
Δ^9-THC	6.77 ± 0.05 (171)	50 ± 11	-	32 ± 1 at 30 μM	-
CP 55,490	7.98 ± 0.04 (10.4)	100 ± 2	7.64 ± 0.06 (22.9)	92 ± 9	2.2
CUMYL-BICA (**8**)	8.10 ± 0.14 (8.0)	109 ± 5	7.61 ± 0.20 (24.5)	101 ± 7	3.1
CUMYL-PICA (**9**)	8.38 ± 0.04 (4.2)	116 ± 2	7.23 ± 0.09 (58.4)	102 ± 5	14
CUMYL-5F-PICA (**10**)	8.55 ± 0.05 (2.8)	118 ± 2	7.40 ± 0.10 (39.6)	104 ± 5	14
CUMYL-FUBICA (**11**)	7.91 ± 0.10 (12.3)	112 ± 5	7.34 ± 11 (45.5)	92 ± 5	3.7

CUMYL-CHMICA (**12**)	8.02 ± 0.13 (9.5)	120 ± 5	6.91 ± 0.22 (122)	92 ± 9	13
CUMYL-BINACA (**13**)	8.81 ± 0.10 (1.6)	109 ± 3	7.92 ± 0.04 (12.0)	89 ± 2	7.5
CUMYL-PINACA (**14**)	8.64 ± 0.08 (2.3)	116 ± 3	6.97 ± 0.13 (107)	106 ± 6	47
CUMYL-5F-PINACA (**15**)	9.37 ± 0.06 (0.43)	110 ± 3	7.95 ± 0.09 (11.3)	87 ± 3	26
CUMYL-FUBINACA (**16**)	8.73 ± 0.06 (1.8)	108 ± 3	7.63 ± 0.12 (23.7)	84 ± 5	13
CUMYL-CHMINACA (**17**)	8.76 ± 0.12 (1.7)	112 ± 4	7.05 ± 0.14 (90.0)	84 ± 5	53

*CB_1 selectivity expressed as the ratio of CB_1 EC_{50} to CB_2 EC_{50}.

All cumyl-derived SCs **8**–**17** activated CB_1 and CB_2 receptors. All compounds, except CUMYL-FUBICA (EC_{50} = 12.3 nM) had greater potency (0.43–9.5 nM) than CP 55,940 (10.4 nM) for CB_1 receptor-mediated activation of GIRK. Compounds **8**–**17** also had maximal effects that were comparable to, or greater than, CP 55,940 at CB_1 receptors (108–120%), indicating that these SCs are high efficacy, full agonists. All SCs showed a preference for CB_1 receptors over CB_2 receptors, ranging from low (e.g. CUMYL-BICA, **8**; 3.1 times) to moderate (e.g. CUMYL-CHMINACA, **17**; 52.9 times).

The cumyl-derived indazoles **13**–**17** (EC_{50} = 0.43–2.3 nM) were all more potent CB1 agonists than indoles **8**–**12** (EC_{50} = 2.8–12.3 nM). No clear structure-activity relationships were evident for the nature of the 1-substituent on CB1 potency in SCs **8**–**17**, however, it is noteworthy that a 5-fluoropentyl chain conferred the greatest potency within both the indole (**10**; EC_{50} = 2.8 nM) and indazole (**15**; EC_{50} = 0.43 nM) series. Selectivity for CB_1 over CB_2 was greatest for cumyl-

derivatives featuring a pentyl, 5-fluoropentyl, or (cyclohexyl)methyl group at the 1-position in the indole (13 to 14 times) and indazole (26 to 53 times) series. Conversely, a butyl or 4-fluorobenzyl group in the same position conferred lower levels of selectivity within the indole (3.1 and 3.7 times, respectively) and indazole (7.5 and 13 times, respectively) SCs.

Having shown that **8**–**17** were potent and efficacious cannabimimetic agents *in vitro*, we sought to demonstrate the activity of several of these cumyl-derived SCs *in vivo*. The *in vivo* activity of CUMYL-PICA (**9**) and CUMYL-5F-PICA (**10**) were compared using biotelemetry in rats to provide information regarding the activity of these newer SCs in a living system.

A recent study published as this work was being finalized reported the functional activity of a subset of the compounds reported here in an assay of G protein activation (GTPγS binding).[10] There are significant differences in the rank order of potency and CB1 selectivity reported between the 2 studies (SI Table 2). Strikingly, we found CUMYL-5F-PINACA to be 20 fold more potent than CP 55,940 at CB1, while it was 20 times less potent than CP 55,940 in the GTPγS assay. We also found that CUMYL-PINACA had a 50-fold preference for CB1 over CB2, while in the GTPγS assay, CUMYL-PINACA was reported as CB2 preferring by 10 fold. The CP 55,940 selectivity for CB1 over CB2 was broadly similar in both studies – 2.2 fold for GIRK, 0.65 fold for GTPγS, and may reflect relative differences in receptor expression. It is also notable that in the GIRK assay CUMYL-PINACA, CUMYL-PICA and CUMYL-5F-PICA has maximal responses 15-20 % higher than those of CP 55,940, suggesting a higher efficacy. The GTPγS assay is good for determining relative efficacy as the maximal response is usually unconstrained, unfortunately the details of the relative maximal responses for these drugs were

not reported by Asada et al.[10] Overall, details of the GTPγS assay are sparsely reported, without even identification of the cell types used, but the striking differences in the results between the 2 assays may reflect an unappreciated signaling bias by this class of SCs. The assays are also very different in that GIRK activation represents a transient maximal signal likely to be unaffected by receptor regulation, while GTPγS assays are typically accumulation assays that are carried out over extended time in broken cell preparations.

In rodents, cross-substitution of aroylindole SCs, like JWH-018, and phytocannabinoid Δ^9-THC has been demonstrated, indicating that these cannabinoids produce similar pharmacological effects despite structural heterogeneity.[11-20] Cannabinoids induce bradycardia, hypothermia, and hypolocomotion in mice and rats, and these physiological changes are common to functional cannabinoids from disparate structural classes.[21] We have previously determined the hypothermic and bradycardic potencies of Δ^9-THC and numerous structurally diverse SCs, including JWH-018, AM-2201, UR-144, XLR-11, APICA, STS-135, PB-22, 5F-PB-22, AB-PINACA, and AB-FUBINACA in rats.[22-26] The cannabimimetic activities of CUMYL-PICA and CUMYL-5F-PICA were assessed using radiotelemetry in male Long Evans rats, and the effects of these SCs on body temperature (Fig. 5) and heart rate (Fig. 6) are presented below.

Rat body temperature from 1 hour prior to intraperitoneal (i.p.) injection to 6 hours post injection of CUMYL-PICA and CUMYL-5F-PICA are presented in 15 minute bins in Figure 5. The dashed line on the figures represents the time of SC injection. Each SC was investigated using a cohort of 4 rats, with a different cohort used for the two compounds. Doses were escalated from

0 mg/kg (baseline) to 0.1, 0.3, and 1.0 mg/kg for each compound with at least 2 washout days with no injections between each dose.

Both CUMYL-PICA and CUMYL-5F-PICA evoked a pronounced hypothermic effect at 1 mg/kg compared to vehicle during the 6 h immediately following injection (CUMYL-PICA $P < .001$; CUMYL-5F-PICA $P < 0.0001$; Fig. 5), analyzed via a two-way mixed-model ANOVA. At 0.3 mg/kg, neither compound produced a statistically significant hypothermic effect over the 6 h post-injection, although there was some evidence of marginal, brief effects during the first hour. The peak reduction in body temperature at 1 mg/kg was generally greater with CUMYL-5F-PICA (>3 °C) than CUMYL-PICA (>2 °C). When compared to 1 mg/kg of CUMYL-PICA, an equivalent dose of CUMYL-5F-PICA induced a longer hypothermic period, with mean core body temperature returning to baseline roughly 4.5 h post-injection, compared to approximately 2.5 h for CUMYL-PICA.

These results are in agreement with previously reported hypothermia produced by a single 3 mg/kg dose of CUMYL-PICA and CUMYL-5F-PICA in rats, measured periodically via rectal thermometer.[27] Taken together, these results indicate that both compounds produce hypothermia in rats in a dose-dependent manner at doses of 1 mg/kg and higher.

Figure 5. Effects of (a) CUMYL-PICA and (b) CUMYL-5F-PICA on rat body temperature. Dashed line denotes time of intraperitoneal injection. Each point represents the mean ± SEM for four animals.

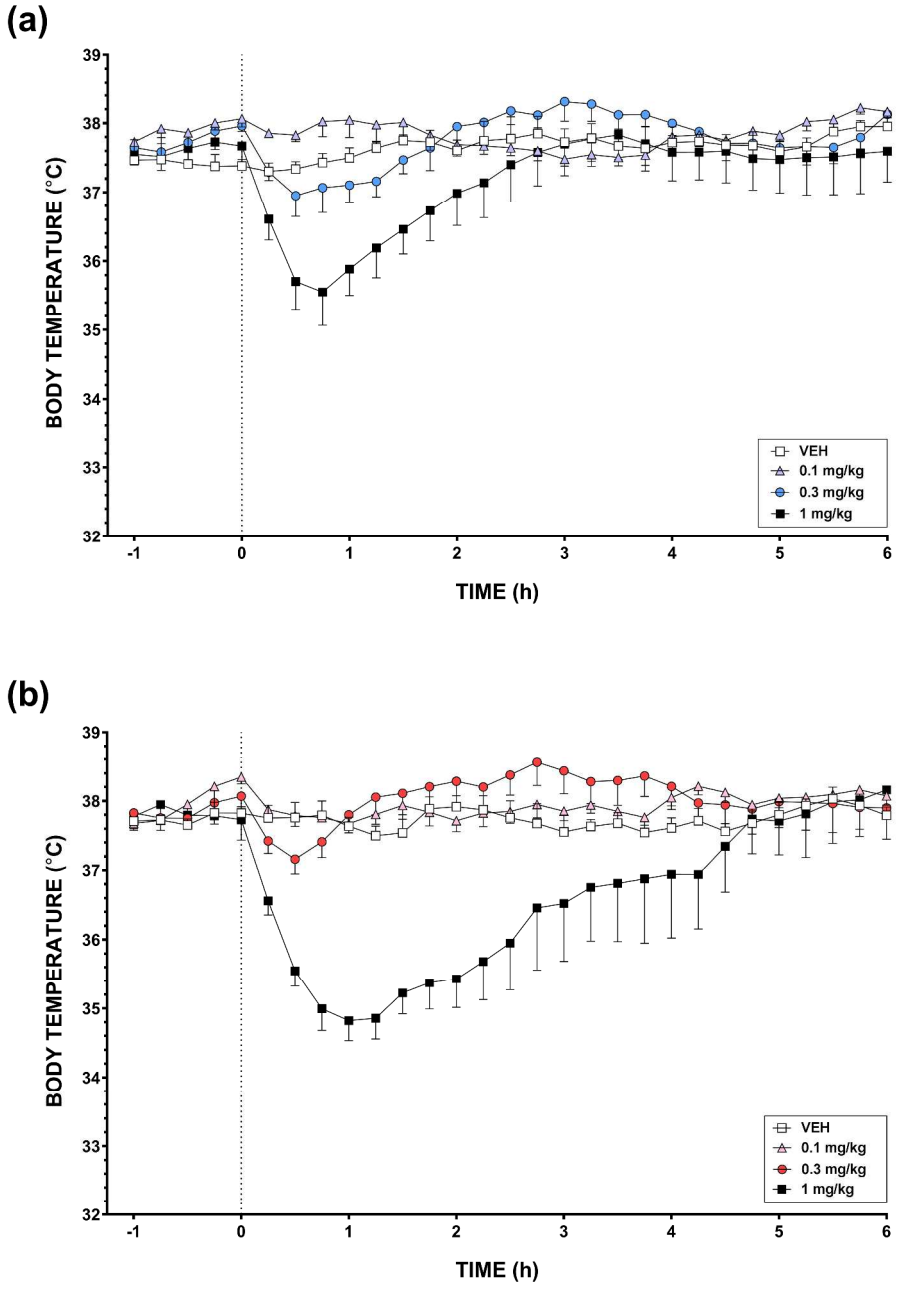

Changes in heart rate effected by CUMYL-PICA and CUMYL-5F-PICA are presented in Fig. 6. Although heart rate data was more variable than body temperature data, analysis using a two-way mixed-model ANOVA showed that CUMYL-PICA significantly reduced heart-rate over the

6 h immediately following doses of 0.3 mg/kg ($P < 0.05$) and 1 mg/kg ($P < 0.01$). CUMYL-5F-PICA significantly reduced heart rate following a dose of 1 mg/kg ($P < .01$) only.

Figure 6. Effects of (a) CUMYL-PICA and (b) CUMYL-5F-PICA on rat heart rate. Dashed line denotes time of intraperitoneal injection. Each point represents the mean ± SEM for four animals.

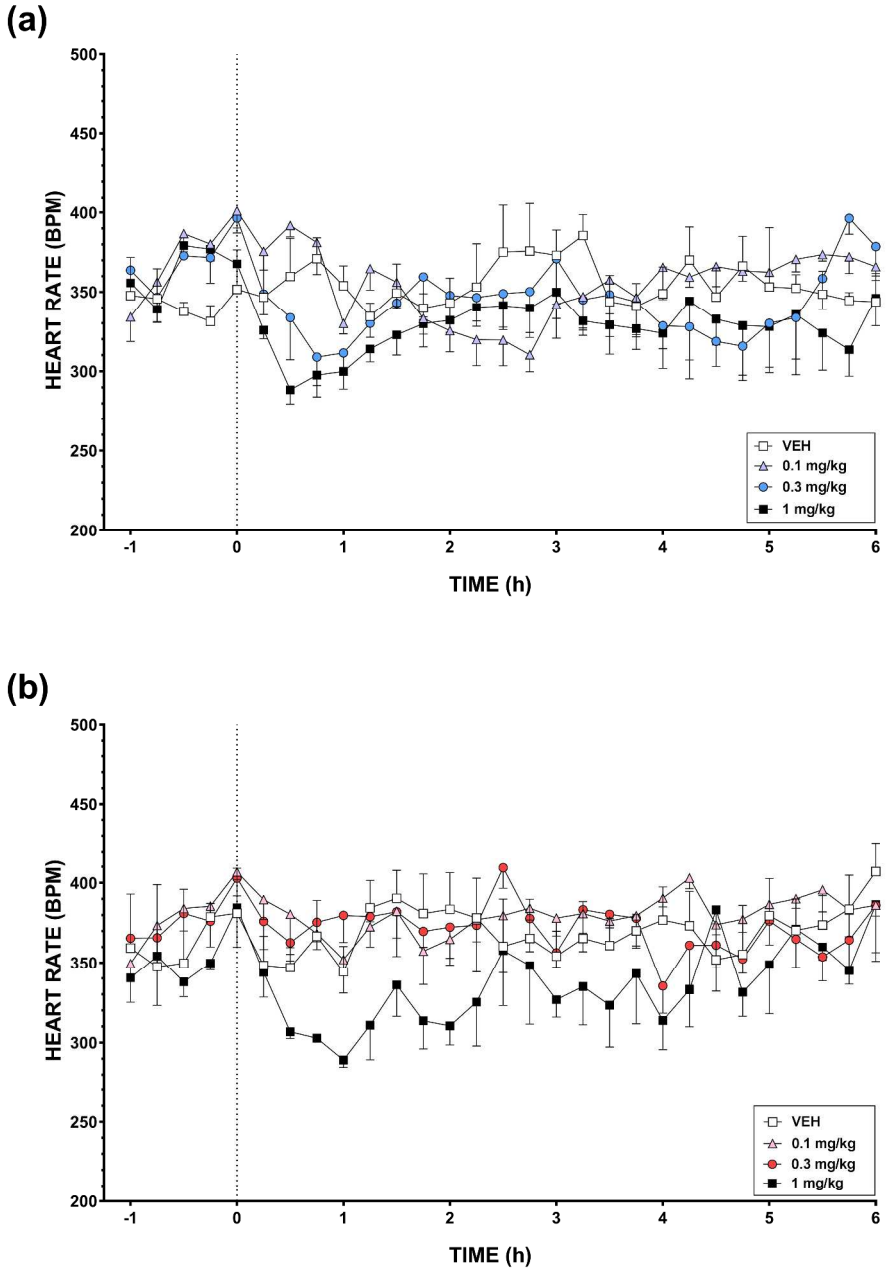

To confirm that the observed effects were mediated through CB_1 or CB_2 receptors, we assessed the reversibility of the effects of CUMYL-PICA and CUMYL-5F-PICA on body temperature in rats following pretreatment with either CB_1 receptor antagonist rimonabant (SR141716) or CB_2 receptor antagonist SR144528 (Fig. 7). The hypothermic effect of 1 mg/kg CUMYL-PICA and

CUMYL-5F-PICA was strongly attenuated by pre-treatment with rimonabant (all $p < .001$, Fig. S21, Supporting Information). No attenuation of hypothermia was observed following pre-treatment with SR144528 for either compound. This indicates a selective CB_1 receptor dependent hypothermic mechanism. We have reported similar CB_1 receptor dependence for the hypothermic effects of AB-PINACA, AB-FUBINACA, 5F-AMB, and MDMB-FUBINACA.[24, 26]

Figure 7. Effects of (a) 1 mg/kg CUMYL-PICA or (b) 1 mg/kg CUMYL-5F-PICA on rat body temperature following pretreatment (30 min prior) with vehicle solution (VEH), 3 mg/kg rimonabant (CB_1 antagonist), or 3 mg/kg SR144528 (CB_2 antagonist). The first dashed line denotes time of pretreatment injection (vehicle or antagonist). The second dashed line denotes time of vehicle or SC injection. Each point represents the mean ± SEM for four animals.

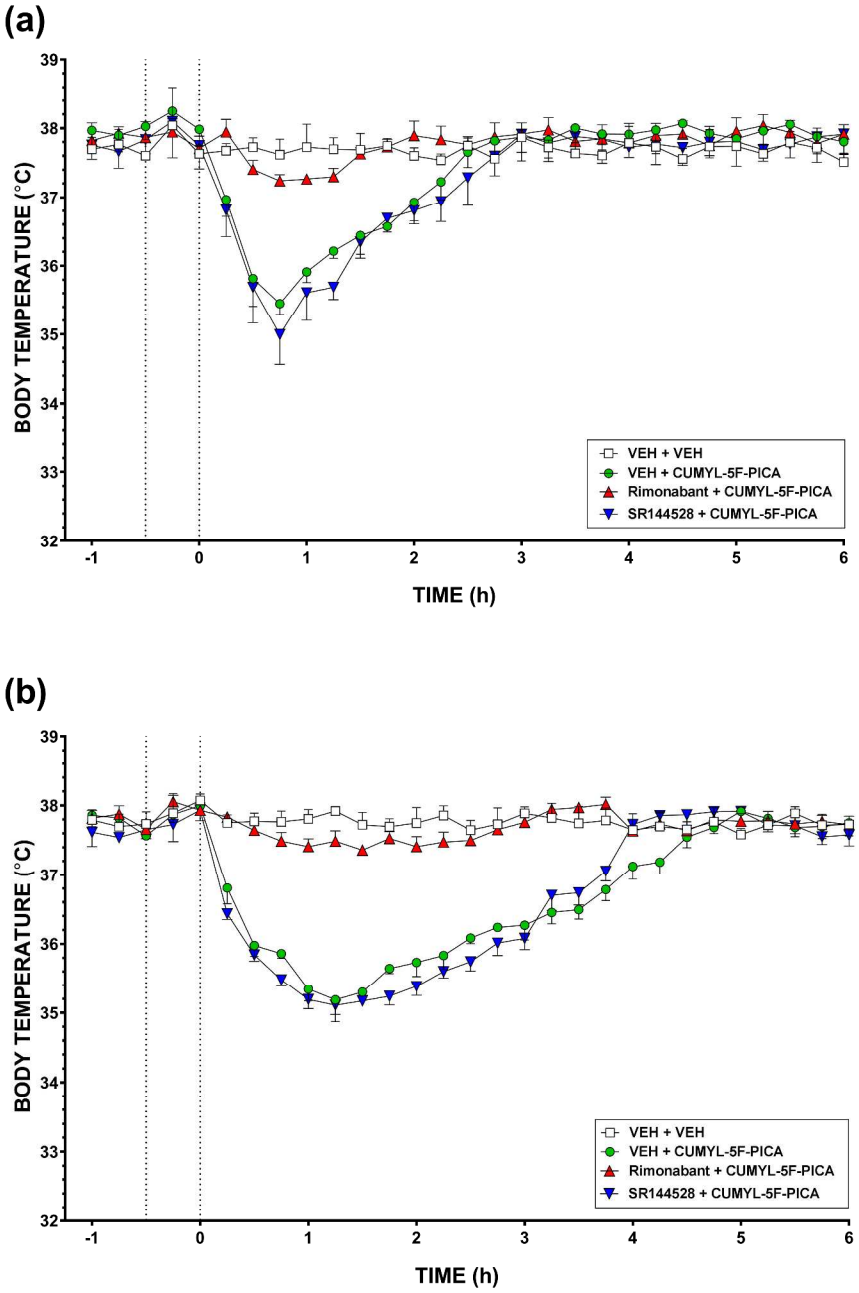

Conclusion: As the structural heterogeneity of SCs continues to increase, the rapid chemical and pharmacological characterization of emergent analogues remains crucial to effective responses by law enforcement agencies and policy makers. Here we have provided the systematic evaluation of a series of *N*-cumyl-1-alkyl-1*H*-ind(az)ole-3-carboxamide SCs of forensic interest,

including CUMYL-BICA, CUMYL-PICA, CUMYL-5F-PICA, CUMYL-PINACA, CUMYL-5F-PINACA, and related analogues. The described synthetic method is general, and should provide forensic chemists with access to newer cumyl-derived analogues featuring alternative substituents in the 1-position. All synthesized SCs were potent agonists of CB_1 and CB_2 receptors in a FLIPR membrane potential assay, thereby classifying them as functional cannabinoids. As with earlier series of related SCs, the indazole analogues were generally more potent CB_1 agonists than the corresponding indole congeners. CUMYL-PICA and CUMYL-5F-PICA produced significant hypothermic and bradycardic effects in rats at doses of 1 mg/kg, and the former were reversed by pretreatment with CB_1 antagonist rimonabant (but not CB_2 antagonist SR144528), suggesting CB_1-mediated effects. The *in vitro* and *in vivo* data indicate that *N*-cumyl-1-alkyl-1*H*-ind(az)ole-3-carboxamide SCs are potent cannabinoids with likely central activity at CB_1.

Materials and methods

General chemical synthesis details

The synthesis of **8**–**17** is shown in Figures 3 and 4. All reactions were performed under an atmosphere of nitrogen or argon unless otherwise specified. Anhydrous tetrahydrofuran (THF), methanol, acetonitrile, and dimethyl sulfoxide (DMSO) (SigmaAldrich, St. Louis, MO, USA) were used as purchased. Commercially available chemicals (Sigma-Aldrich) were used as purchased. Analytical thin-layer chromatography was performed using Merck aluminum-backed silica gel 60 F254 (0.2 mm) plates (Merck, Darmstadt, Germany), which were visualized using

shortwave (254 nm) UV fluorescence. Flash chromatography was performed using Merck Kieselgel 60 (230–400 mesh) silica gel. Melting point ranges (m.p.) were measured in open capillaries using a Stuart SMP10 melting point apparatus (Bibby Scientific, Staffordshire, UK) and are uncorrected. Nuclear magnetic resonance spectra were recorded at 300 K using either a Bruker AVANCE DRX300 (300 MHz) spectrometer (Bruker, Bremen, Germany). The data for ^{1}H NMR spectra are reported as chemical shift (δ ppm) relative to the residual protonated solvent resonance, relative integral, multiplicity (s = singlet, br s = broad singlet, d = doublet, t = triplet, quat. = quartet, quin. = quintet, m = multiplet), coupling constants (J Hz) and assignment. The data for ^{13}C NMR spectra are reported as chemical shift (δ ppm) relative to residual solvent. Assignment of signals was assisted by correlation spectroscopy (COSY), distortionless enhancement by polarization transfer (DEPT), heteronuclear single quantum coherence (HSQC), and heteronuclear multiple-bond correlation (HMBC) experiments where necessary. Low-resolution mass spectra (LRMS) was recorded using electrospray ionization (ESI) recorded on a Finnigan LCQ ion trap mass spectrometer (ThermoFisher Scientific, Waltham, MA, USA). High-resolution mass spectra (HRMS) were run on a Bruker 7T Apex Qe Fourier Transform Ion Cyclotron resonance mass spectrometer equipped with an Apollo II ESI/APCI/MALDI Dual source by the Mass Spectrometry Facility of the School of Chemistry at the University of Sydney. IR absorption spectra were recorded on a Bruker ALPHA FT-IR spectrometer as solid or thin film from ethanol, and the data are reported as vibrational frequencies (cm^{-1}). Please see the supplementary material for detailed chemical synthesis and ^{1}H and ^{13}C NMR spectra of all final compounds.

General procedure A: Amidation of 1-substituted-1*H*-indole-3-carboxylic acids and 1-substituted-1*H*-indazole-3-carboxylic acids (8–17). To a solution of the appropriate 1-substituted-1*H*-indole-3-carboxylic acid or 1-substituted-1*H*-indazole-3-carboxylic acid (0.39 mmol), cumylamine (60 μL, 0.41 mmol, 1.05 equiv.), EDC·HCl (150 mg, 0.78 mmol, 2.0 equiv.) and HOBt (119 mg, 0.78 mmol, 2.0 equiv.) in DMSO (5 mL) was added DIPEA (340 μL, 1.95 mmol, 5.0 equiv.) dropwise and the mixture was stirred for 14 h. The reaction was quenched by the addition of sat. aq. $NaHCO_3$ (75 mL) and extracted with EtOAc (3 × 75 mL). The combined organic layers were washed with brine (100 mL), dried ($MgSO_4$), and evaporated under reduced pressure. The pure amides were obtained following purification by flash chromatography.

General procedure B: Synthesis of 1-(1-substituted-1*H*-indol-3-yl)-2,2,2-trifluoroethanones (19–23). To a cooled (0 °C) suspension of sodium hydride (60% dispersion in mineral oil, 137 mg, 3.42 mmol, 2.0 equiv.) in DMF (6 mL) was added indole (200 mg, 1.71 mmol) portionwise and the mixture stirred for 10 min. The mixture was treated dropwise with the appropriate bromoalkane (1.80 mmol, 1.05 equiv.) and stirred at ambient temperature for 1 h. The cooled (0 °C) mixture was treated dropwise with trifluoroacetic anhydride (600 μL, 4.28 mmol, 2.5 equiv.) and stirred at ambient temperature for 1 h. The reaction was poured into ice water (75 mL) and extracted with CH_2Cl_2 (3 x 75 mL). The combined organic extracts were washed with H_2O (100 mL), brine (100 mL), dried ($MgSO_4$) and the solvent evaporated under reduced pressure. The pure 1-alkyl-3-trifluoroacetylindoles were obtained following purification by flash chromatography.

General procedure C: Synthesis of 1-substituted-1*H*-indole-3-carboxylic acids and 1-alkyl-1*H*-indazole-3-carboxylic acids (24–28 and 35–39). To a solution of the appropriate 1-substituted-3-(trifluoroacetyl)indole or methyl 1-substittued-1*H*-indazole-3-carboxylate (2.58 mmol) in MeOH (20 mL) was added 1 M aq. NaOH (3.87 mL, 3.87 mmol, 1.5 equiv.) and the solution heated at reflux for 18 h. The mixture was cooled to ambient temperature, solvent was evaporated in vacuo, and the mixture was poured onto sat. aq. $NaHCO_3$ (75 mL). The aqueous phase was washed with Et_2O (75 mL) and the pH adjusted to 2 with 1 M aq. HCl. The aquoeus phase was extracted with Et_2O (3 × 75 mL) and the combined organic layers were washed with brine (150 mL), dried ($MgSO_4$) and concentrated *in vacuo* to give the crude products. Analytical purity for 1-substituted-1*H*-indazole-3-carboxylic acids was achieved by recrystallization from *i*-PrOH.

General procedure D: Synthesis of methyl 1-substituted-1*H*-indazole-3-carboxylates (30–34). To a cooled (0 °C) solution of methyl 1*H*-indazole-3-carboxylate (**29**, 500 mg, 2.84 mmol) in THF (15 mL) was added potassium *tert*-butoxide (350 mg, 3.12 mmol, 1.1 equiv.), and the mixture warmed to ambient temperature and stirred for 1 h. The cooled (0 °C) mixture was treated dropwise with the appropriate bromoalkane (2.98 mmol, 1.05 equiv.) and stirred for 48 h. The reaction was quenched by pouring onto H_2O (100 mL) and the layers separated. The aqueous phase was extracted with EtOAc (3 × 100 mL), and the combined organic layers were washed with brine (150 mL), dried ($MgSO_4$), and the solvent evaporated under reduced pressure. The crude materials were purified by flash chromatography.

In vitro pharmacological evaluation of compounds 8–17. Mouse AtT-20 neuroblastoma cells stably transfected with human CB_1 or human CB_2 have been previously described[26] and were cultured in Dulbecco's modified Eagle's medium (DMEM) containing 10% fetal bovine serum (FBS), 100 U penicillin/streptomycin, and 300 μg/ml G418. Cells were passaged at 80% confluency as required. Cells for assays were grown in 75 cm^2 flasks and used at 90% confluence. The day before the assay cells were detached from the flask with trypsin/EDTA (Sigma-Aldrich) and resuspended in 10 ml of Leibovitz's L-15 media supplemented with 1% FBS, 100 U penicillin/streptomycin and 15 mM glucose (membrane potential assay and Ca5 calcium assay). The cells were plated in volume of 90 μl in black walled, clear bottomed 96-well microplates (Corning, Oneonta, NY, USA) which had been precoated with poly-L-lysine (Sigma-Aldrich). Cells were incubated overnight at 37 °C in ambient CO_2.

Membrane potential was measured using a FLIPR membrane potential assay kit (blue) from Molecular Devices (Sunnyvale, CA, USA), as described previously [28]. The dye was reconstituted with assay buffer of composition (mM): NaCl 145, HEPES 22, Na_2HPO_4 0.338, $NaHCO_3$ 4.17, KH_2PO_4 0.441, $MgSO_4$ 0.407, $MgCl_2$ 0.493, $CaCl_2$ 1.26, glucose 5.56, bovine serum albumin (pH 7.4, osmolarity 315 ± 5). Prior to the assay, cells were loaded with 90 μl/well of the dye solution without removal of the L-15, giving an initial assay volume of 180 μl/well. Plates were then incubated at 37 °C at ambient CO_2 for 60 min. Fluorescence was measured using a FlexStation 3 (Molecular Devices) microplate reader with cells excited at a wavelength of 530 nm and emission measured at 565 nm. Baseline readings were taken every 2 s for at least 60 s, at which time either drug or vehicle was added in a volume of 20 μl. The background fluorescence of cells without dye or dye without cells was negligible. Changes in fluorescence were expressed

as a percentage of baseline fluorescence after subtraction of the changes produced by vehicle addition. The final concentration of dimethyl sulfoxide was always 0.1%.

Data were analyzed with PRISM (GraphPad Software Inc., San Diego, CA), using four-parameter nonlinear regression to fit concentration-response curves. In all plates, a maximally effective concentration of CP 55,940 (Cayman Chemical, Ann Arbor, MI, USA) was added to allow for normalization between assays.

In vivo pharmacological evaluation of CUMYL-PICA and CUMYL-5F-PICA. Two cohorts of 4 adult male Long Evans rats (Animal Resources Centre, Perth, Australia) initially weighing between 174 and 192 g were used for biotelemetric assessment of body temperature and heart rate changes following each compound. The rats were singly housed in an air-conditioned testing room (22 ± 1 °C) on a 12 h reverse light/dark cycle (lights on from 21:00 to 09:00). Standard rodent chow and water were provided ad libitum. All experiments were approved by The University of Sydney Animal Ethics Committee.

Biotelemetry transmitters (TA11CTA-F40, Data Sciences International, St. Paul, MN) were implanted as previously described.[26] Briefly, following anaesthetization (isoflurane, 3% induction, 2% maintenance) a biotelemetry transmitter (TA11CTA-F40, Data Sciences International, St. Paul, MN) was placed in the peritoneal cavity according to the manufacturers protocol. The wound was sutured closed and the rats were allowed one week of recovery before data collection.

The rats were habituated over multiple days to injections of vehicle solution (5% EtOH, 5% Tween 80, 90% physiological saline) at a set time of day (10:00 am). Each cohort then received injections of each compound at the same time of day in an ascending dose sequence (0.1, 0.3, 1, mg/kg). This ascending sequence reduces the risk posed to the animals in assessing hitherto untested compounds. Two washout days were given between each dose.

For the antagonist studies (Fig. 7), a third and fourth cohort of drug-naïve rats were used for each compound (weight range 169–199 g). Each cohort received injections of either vehicle, CB_1 antagonist (rimonabant, 3 mg/kg), or CB_2 antagonist (SR144528, 3 mg/kg), followed by CUMYL-PICA (1 mg/kg) or CUMYL-5F-PICA (1 mg/kg). The order of treatments was counterbalanced within each cohort. The vehicle or antagonist injections were given to rats 30 minutes prior to the CUMYL-PICA or 5F-CUMYL-PICA injections.

Data for heart rate and body temperature was gathered continuously at 1000 Hz and organized into 15 minute bins using Dataquest A.R.T. software (version 4.3, Data Sciences International, St. Paul, MN), and analysed using Prism (version 7.00, GraphPad Software Inc., San Diego, CA). Hypothermic and bradycardic effects were analysed using a two-way mixed-model ANOVA. Main effects of each dose of CUMYL-PICA or CUMYL-5F-PICA were compared to vehicle using planned Dunnet's contrasts.

For the antagonist studies, we calculated the area between baseline and drug-treatment body temperature curves for each rat as a measure of antagonist efficacy. Briefly, for any time point,

the area between baseline data points (B_t) and drug-treatment data points (D_t) and the subsequent time points (B_{t+1} and D_{t+1}) forms a trapezoid, the area of which can be calculated via the formula:

$$Area = \frac{(B_t - D_t) + (B_{t+1} - D_{t+1})}{2}$$

The area between the vehicle-vehicle baseline and the vehicle-SC (i.e. vehicle-CUMYL-PICA or vehicle-CUMYL-5F-PICA), rimonabant-SC and SR144528-SC treatments was calculated over a 6 h time period post-injection of SC. These areas were analyzed using a one-way repeated measure ANOVA with planned Dunnet's contrasts comparing the antagonist areas to the vehicle-SC area.

Acknowledgments

Work was supported by NHMRC Project Grant 1107088 awarded to M.K., I.S.M., and M.C.

Supporting Information

Table S1: Names, CAS numbers, and references for selected compounds (pp. 2–3).
Figures S1–S20: ^{1}H and ^{13}C NMR spectra for selected compounds (pp. 4–23).
Table S2: Hyperpolarization of AtT-20 cells expressing CB_1 or CB_2 by CP 55,940 or 8-17 with and without pertussis toxin (PTX) pretreatment (pp. 24).
Figure S21: Mean area under the vehicle-vehicle baseline curve (AUC ± SEM) for body temperature for CUMYL-PICA and CUMYL-5F-PICA, following pretreatment with vehicle, rimonabant (CB_1 antagonist), or SR144528 (CB_2 antagonist) (pp. 25).
Table S3: Comparison of the potency of selected CUMYL- drugs at human CB1 and CB2 receptors measured using activation of GIRK or stimulation of $GTP_{\gamma}S$ binding (Asada et al., 2017) (pp.26).

References

1. UNODC, World Drug Report 2017.
2. Qian, Z.; Hua, Z.; Liu, C.; Jia, W., Four types of cannabimimetic indazole and indole derivatives, ADB-BINACA, AB-FUBICA, ADB-FUBICA, and AB-BICA, identified as new psychoactive substances. *Forensic toxicology* **2016,** *34*, 133-143.
3. Shevyrin, V.; Melkozerov, V.; Eltsov, O.; Shafran, Y.; Morzherin, Y., Synthetic cannabinoid 3-benzyl-5-[1-(2-pyrrolidin-1-ylethyl)-1*H*-indol-3-yl]-1,2,4-oxadiazole. The first detection in illicit market of new psychoactive substances. *Forensic Science International* **2016,** *259*, 95-100.
4. Adams, A. J.; Banister, S. D.; Irizarry, L.; Trecki, J.; Schwartz, M.; Gerona, R., "Zombie" Outbreak Caused by the Synthetic Cannabinoid AMB-FUBINACA in New York. *N Engl J Med* **2017,** *376* (3), 235-242.
5. Bowden, M. J.; Williamson, J. P. B. Cannabinoid Compounds. WO2014167530A1, 2014.
6. EMCDDA *EMCDDA–Europol 2014 Annual Report on the implementation of Council Decision 2005/387/JHA*; 2015.
7. Dobaja, M.; Grenc, D.; Kozelj, G.; Brvar, M., Occupational transdermal poisoning with synthetic cannabinoid cumyl-PINACA. *Clin Toxicol (Phila)* **2017,** *55* (3), 193-195.
8. Abouchedid, R.; Hudson, S.; Thurtle, N.; Yamamoto, T.; Ho, J. H.; Bailey, G.; Wood, M.; Sadones, N.; Stove, C. P.; Dines, A.; Archer, J. R. H.; Wood, D. M.; Dargan, P. I., Analytical confirmation of synthetic cannabinoids in a cohort of 179 presentations with acute recreational drug toxicity to an Emergency Department in London, UK in the first half of 2015. *Clin Toxicol (Phila)* **2017,** *55* (5), 338-345.
9. Longworth, M.; Banister, S. D.; Mack, J. B. C.; Glass, M.; Connor, M.; Kassiou, M., The 2-alkyl-2H-indazole regioisomers of synthetic cannabinoids AB-CHMINACA, AB-FUBINACA, AB-PINACA, and 5F-AB-PINACA are possible manufacturing impurities with cannabimimetic activities. *Forensic toxicology* **2016,** *34* (2), 286-303.
10. Asada, A.; Doi, T.; Tagami, T.; Takeda, A.; Satsuki, Y.; Kawaguchi, M.; Nakamura, A.; Sawabe, Y., Cannabimimetic activities of cumyl carboxamide-type synthetic cannabinoids. *Forensic toxicology* **2017**. doi 10.1007/s11419-017-0374-9.

11. Wiley, J. L.; Marusich, J. A.; Martin, B. R.; Huffman, J. W., 1-Pentyl-3-phenylacetylindoles and JWH-018 share in vivo cannabinoid profiles in mice. *Drug Alcohol Depen.* **2012,** *123* (1-3), 148-153.

12. Wiley, J. L.; Marusich, J. A.; Lefever, T. W.; Grabenauer, M.; Moore, K. N.; Thomas, B. F., Cannabinoids in disguise: Δ9-tetrahydrocannabinol-like effects of tetramethylcyclopropyl ketone indoles. *Neuropharmacology* **2013,** *75*, 145-154.

13. Gatch, M. B.; Forster, M. J., Δ9-Tetrahydrocannabinol-like discriminative stimulus effects of compounds commonly found in K2/Spice. *Behav. Pharmacol.* **2014,** *25* (8), 750-757.

14. Wiley, J. L.; Lefever, T. W.; Cortes, R. A.; Marusich, J. A., Cross-substitution of Δ9-tetrahydrocannabinol and JWH-018 in drug discrimination in rats. *Pharmacol. Biochem. Behav.* **2014,** *124*, 123-128.

15. Gatch, M. B.; Forster, M. J., Δ9-Tetrahydrocannabinol-like effects of novel synthetic cannabinoids found on the gray market. *Behav. Pharmacol.* **2015,** *26* (5), 460-468.

16. Wiley, J. L.; Marusich, J. A.; Lefever, T. W.; Antonazzo, K. R.; Wallgren, M. T.; Cortes, R. A.; Patel, P. R.; Grabenauer, M.; Moore, K. N.; Thomas, B. F., AB-CHMINACA, AB-PINACA, and FUBIMINA: Affinity and Potency of Novel Synthetic Cannabinoids in Producing Δ9-Tetrahydrocannabinol-Like Effects in Mice. *J. Pharmacol. Exp. Ther.* **2015,** *354* (3), 328-339.

17. Gatch, M. B.; Forster, M. J., Δ(9)-Tetrahydrocannabinol-like effects of novel synthetic cannabinoids in mice and rats. *Psychopharmacology (Berl.)* **2016,** *233* (10), 1901-1910.

18. Wiley, J. L.; Lefever, T. W.; Marusich, J. A.; Grabenauer, M.; Moore, K. N.; Huffman, J. W.; Thomas, B. F., Evaluation of first generation synthetic cannabinoids on binding at non-cannabinoid receptors and in a battery of in vivo assays in mice. *Neuropharmacology* **2016,** *110* (Pt A), 143-153.

19. Thomas, B. F.; Lefever, T. W.; Cortes, R. A.; Grabenauer, M.; Kovach, A. L.; Cox, A. O.; Patel, P. R.; Pollard, G. T.; Marusich, J. A.; Kevin, R. C.; Gamage, T. F.; Wiley, J. L., Thermolytic Degradation of Synthetic Cannabinoids: Chemical Exposures and Pharmacological Consequences. *J. Pharmacol. Exp. Ther.* **2017,** *361* (1), 162-171.

20. Wiley, J. L.; Lefever, T. W.; Marusich, J. A.; Craft, R. M., Comparison of the discriminative stimulus and response rate effects of Δ9-tetrahydrocannabinol and synthetic cannabinoids in female and male rats. *Drug Alcohol Depend* **2017,** *172*, 51-59.

21. Wiley, J. L.; Marusich, J. A.; Huffman, J. W., Moving around the molecule: Relationship between chemical structure and in vivo activity of synthetic cannabinoids. *Life Sci.* **2014,** *97* (1), 55-63.

22. Banister, S. D.; Wilkinson, S. M.; Longworth, M.; Stuart, J.; Apetz, N.; English, K.; Brooker, L.; Goebel, C.; Hibbs, D. E.; Glass, M.; Connor, M.; McGregor, I. S.; Kassiou, M., The synthesis and pharmacological evaluation of adamantane-derived indoles: cannabimimetic drugs of abuse. *ACS Chem. Neurosci.* **2013,** *4* (7), 1081-1092.

23. Banister, S. D.; Stuart, J.; Kevin, R. C.; Edington, A.; Longworth, M.; Wilkinson, S. M.; Beinat, C.; Buchanan, A. S.; Hibbs, D. E.; Glass, M.; Connor, M.; McGregor, I. S.; Kassiou, M., Effects of Bioisosteric Fluorine in Synthetic Cannabinoid Designer Drugs JWH-018, AM-2201, UR-144, XLR-11, PB-22, 5F-PB-22, APICA, and STS-135. *ACS Chem. Neurosci.* **2015,** *6* (8), 1445-1458.

24. Banister, S. D.; Stuart, J.; Conroy, T.; Longworth, M.; Manohar, M.; Beinat, C.; Wilkinson, S. M.; Kevin, R. C.; Hibbs, D. E.; Glass, M.; Connor, M.; McGregor, I. S.; Kassiou, M., Structure–activity relationships of synthetic cannabinoid designer drug RCS-4 and its regioisomers and C4 homologues. *Forensic toxicology* **2015,** *33* (2), 355-366.

25. Banister, S. D.; Moir, M.; Stuart, J.; Kevin, R. C.; Wood, K. E.; Longworth, M.; Wilkinson, S. M.; Beinat, C.; Buchanan, A. S.; Glass, M.; Connor, M.; McGregor, I. S.; Kassiou, M., Pharmacology of Indole and Indazole Synthetic Cannabinoid Designer Drugs AB-FUBINACA, ADB-FUBINACA, AB-PINACA, ADB-PINACA, 5F-AB-PINACA, 5F-ADB-PINACA, ADBICA, and 5F-ADBICA. *ACS Chem Neurosci* **2015,** *6* (9), 1546-1559.

26. Banister, S. D.; Longworth, M.; Kevin, R.; Sachdev, S.; Santiago, M.; Stuart, J.; Mack, J. C.; Glass, M.; McGregor, I. S.; Connor, M.; Kassiou, M., Pharmacology of Valinate and tert-Leucinate Synthetic Cannabinoids 5F-AMBICA, 5F-AMB, 5F-ADB, AMB-FUBINACA, MDMB-FUBINACA, MDMB-CHMICA, and Their Analogues. *ACS Chem. Neurosci.* **2016,** *7* (9), 1241-1254.

27. Kevin, R. C.; Lefever, T. W.; Snyder, R. W.; Patel, P. R.; Fennell, T. R.; Wiley, J. L.; McGregor, I. S.; Thomas, B. F., In vitro and in vivo pharmacokinetics and metabolism of synthetic cannabinoids CUMYL-PICA and 5F-CUMYL-PICA. *Forensic toxicology* **2017**, 1-15.

28. Knapman, A.; Santiago, M.; Du, Y. P.; Bennallack, P. R.; Christie, M. J.; Connor, M., A continuous, fluorescence-based assay of μ-opioid receptor activation in AtT-20 cells. *J Biomol Screen* **2013,** *18* (3), 269-276.

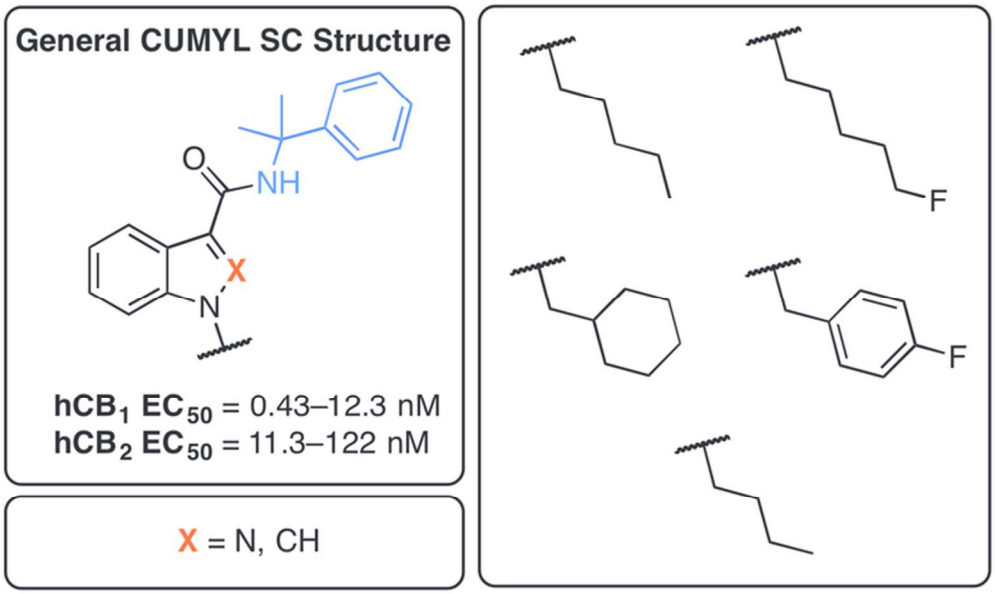

67x40mm (300 x 300 DPI)